crystals

MDPI

Article

Wrinkle-Shaped Nickel Sulfide Grown on Three-Dimensional Nickel Foam: A Binder-Free Electrode Designed for High-Performance Electrochemical Supercapacitor Applications

Sajid Ali Ansari [1,*], Hicham Mahfoz Kotb [1,2] and Mohamad M. Ahmad [1,3]

[1] Department of Physics, College of Science, King Faisal University, P.O. Box 400, Al-Ahsa 31982, Saudi Arabia; hkotb@kfu.edu.sa (H.M.K.); mmohamad@kfu.edu.sa (M.M.A.)
[2] Physics Department, Faculty of Science, Assiut University, Assiut 71516, Egypt
[3] Department of Physics, Faculty of Science, The New Valley University, El-Kharga 72511, Egypt
* Correspondence: sansari@kfu.edu.sa; Tel.: +966-13-589-9598

Abstract: Recently, three-dimensional nickel foam (3D-Nf) has been increasingly studied; however, further modifications in nanoscale surface modification are necessary for particular applications. In this work, three-dimensional hierarchically porous nanogranular NiS (NiS-3D-Nf) and wrinkle-shaped NiS (w-NiS-3D-Nf) structures were fabricated directly on nickel foam by a simple one-step solvothermal process using two different solvents. Several characterization techniques, including X-ray diffraction pattern, X-ray photoelectron spectroscopy, and scanning electron microscopy, were used to characterize the samples' properties. To prove their applicability, supercapacitor electrodes were tested directly in a three-electrode assembly cell. The resulting w-NiS-3D-Nf electrodes exhibited greater capacitive activity than the NiS-3D-Nf electrodes. The optimized w-NiS-3D-Nf electrodes delivered an excellent specific capacitance of 770 Fg^{-1}, at a current density of 1 Ag^{-1}, compared with the NiS-3D-Nf electrodes (162.0 Fg^{-1} @ 1 Ag^{-1}), with a cyclic stability of over 92.67% capacitance retention after 2200 cycles. The resultant unique structure with integrated hierarchical three-dimensional configuration can not only enhance abundant accessible surface areas but also produce strong adhesion to the 3D-Nf, facilitating the fast transportation of ions and electrons for the electrochemical reaction via the conductive 3D-Nf. This set of results suggests that the modification of 3D-Nf surfaces with a suitable solvent has highly significant effects on morphology, and ultimately, electrochemical performance. Additionally, the current preparation approach is simple and worthwhile, and thus offers great potential for supercapacitor applications.

Keywords: supercapacitor; three-dimensional structure; nickel foam; three-electrode; NiS

Citation: Ansari, S.A.; Kotb, H.M.; Ahmad, M.M. Wrinkle-Shaped Nickel Sulfide Grown on Three-Dimensional Nickel Foam: A Binder-Free Electrode Designed for High-Performance Electrochemical Supercapacitor Applications. *Crystals* **2022**, *12*, 757. https://doi.org/10.3390/cryst12060757

Academic Editor: Faxing Wang

Received: 9 May 2022
Accepted: 23 May 2022
Published: 25 May 2022

1. Introduction

The increasing current demand for efficient energy storage devices with high energy/power density has encouraged researchers to develop novel materials and methods, especially in electrochemical energy-storage devices [1]. In this regard, supercapacitors (also known as electrochemical capacitors), are receiving significant attention as prominent power sources and effective substitutes for rechargeable batteries, owing to their superior power density, rapid charge and discharge process, long cyclic stability, and cost-effectiveness, although they suffer from low energy density. Depending on the change storage process, SCs are broadly divided into electric double-layer capacitors (EDLCs), in which energy is stored in collecting charges at the interaction of the electrode and the electrolyte, and pseudocapacitors in which, in addition to the EDLC, the charge storage mechanism is stored through a faradaic redox reaction on the electrode surface [2,3]. It is well known that electrode materials with electrochemical activity and kinetic features are among the key factors in SC performance, along with electrolytes and assembly techniques. In order to obtain effective properties [4], superior electrochemical activity is generally

achieved by means of a proper connection between the active materials and the electrolytes, and rapid ion or electron transportation in the electrode and at the electrode/electrolyte interface. Hence, the design and preparation of electrode materials with high conductivity, specific surface area, and porosity is clearly required [5]. Various metal oxides and hydroxides are broadly investigated as high-performance electrode materials for SCs owing to their rich redox/faradic reactions [6]. Although these types of electrodes exhibit high energy density, they suffer from low inertness and rate capability, and, in particular, their electronic conductivity is insufficient. Nevertheless, the relevant experimental results are generally less acceptable for practical use due to short performance rates and high fabrication costs [5,7]. Therefore, it is necessary to synthesize innovative electrodes that possess suitable electrochemical activity supercapacitors. Considerable efforts have been made to develop the construction of electrodes with high specific capacitance, in order to fabricate supercapacitors with higher energy density.

In order to determine an appropriate structure for the electrodes, researchers' focus has generally been placed on the fabrication of nanostructured materials with various sizes and morphologies, such as nanoflower, nanosheets, nanowires, nanorods, etc., because of their distinctive physico-chemical assets [8,9]. Recently, nanostructured metal sulfides were proven to be among the electrode materials with the greatest potential, and the best alternatives to SCs, because of their highly specific capacitance, suitable semiconductor properties, rich redox capability, cost-effectiveness, and higher electronic conductivity than metal oxides [10,11]. These features of metal sulfides mark them out as suitable electrodes for SC materials, through which they interact with OH ions, leading to reversible redox reactions in electrolytes: $MS + OH^- \leftrightarrow MSOH + e^-$ (M: Co, Ni, etc.) [8]. The reversible redox process enables charge storage and the transmission of electrons/OH ions in active materials.

Among the various metal sulfides, nickel sulfides have attracted immense attention for SC electrodes, owing to their high specific capacitance value, better electrical conductivity, and versatile chemical configuration, along with the fact that they are economical and safe [12,13]. Specifically, their specific capacitance, which is greater than that of carbonaceous-based materials, makes them different from other active materials. The growth/deposition of the electrode material directly on the current collectors is a novel approach to fabricating active electrodes for supercapacitors in order to obtain free-standing, additive- and binder-free hierarchical nanostructure-based electrodes [6,12,13]. In addition, the method (hydrothermal/solvothermal) used for the fabrication of the electrode is stable compared to other methods. For example, at high-temperature fabrication, the crystalline phase is not stable. Materials with high vapor pressure can also be prepared by the hydrothermal method, which offers advantages over other methods [1,9]. This method involves a highly electroactive area, which increases the electrochemical reaction, and it reduces the electrode fabrication process, resulting in the enhancement of the specific capacitance and energy density. Additionally, supercapacitors' activities are also manipulated through the shape/size of electrode materials, as well as their structure. Binder-free supercapacitors have been developed over a decade with a variety of conductive substrates, including carbon fiber paper, stainless steel, titanium foil, silicon foil, and Ni foam [13–15].

Three-dimensional nickel foam is a well-defined and cross-linked network current collector and can be considered a good strategy for the above requirements. Due to its attractive three-dimensional structure and high electronic conductivity, 3D-Nf is widely accepted as a current collector for electrode materials, since it promotes the penetration of electrolytes and ion transport, and improves electrochemical performance. In other words, 3D-Nf fulfils all the requirements of the current collectors and electrodes used to assemble a range of energy-storage devices [13,16]. The use of electrode pastes, which include conductive agents and polymer binders, is an outdated electrode material paste method that hampers electrochemical performance [11]. Hence, growing metal sulfides directly on current collectors is therefore an effective way of enhancing electrochemical performance.

Directly growing NiS on a current collector such as 3D-Nf foam is a viable way to overcome the problems related to poor conductivity and other side effects of binders. In

view of the above findings, a NiS that featured two different solvents in order to obtain two different morphologies was successfully grown directly on nickel foam (NiS-3D-Nf and w-NiS-3D-Nf) by using a simple one-step hydrothermal route to act as a binder-free electrode for pseudocapacitors; the w-NiS-3D-Nf exhibited a high specific capacitance of 770.0 Fg^{-1}, whereas the NiS-3D-Nf delivered a specific capacitance of 162.0 Fg^{-1} at a current density of 1.0 Ag^{-1}, with better cyclic stability (92.67%). We studied the structures and morphologies of the crystals using X-ray diffraction and a scanning electron microscope, respectively. The distinctive wrinkle-shaped morphology of the w-NiS-3D-Nf electrodes and the direct contact between the current collector and the active materials contributed to boosting the electrochemical performance of the prepared electrode.

2. Experimental Procedure

2.1. Materials

Nickel chloride, ethylene glycol, and thiourea were acquired from Sigma Aldrich, whereas the three-dimensional nickel foam was obtained through the MTI Corporation, USA.

2.2. Methods

An X-ray diffractometer (PRO-MPD, Netherlands) was used to examine the phases and crystal structures of the as-synthesized w-NiS-3D-Nf and NiS-3D-Nf. The chemical structure and its interaction with the w-NiS-3D-Nf and NiS-3D-Nf were observed by X-ray photoelectron spectroscopy. The surface morphologies of the w-NiS-3D-Nf and NiS-3D-Nf were examined through field emission scanning electron microscopy (Tecnai; F20-FEI; USA).

2.3. Electrochemical Measurements

The electrochemical measurements, such as cyclic voltammetry (CV) and galvanostatic charge–discharge (GCD), of the w-NiS-3D-Nf and NiS-3D-Nf electrodes were examined on a VersaSTAT 3 potentiostat electrochemical workstation equipped with PC. The Ag/AgCl electrode was used as reference electrode and Pt plate was used as counter electrode, whereas the w-NiS-3D-Nf and NiS-3D-Nf electrodes were used as working electrodes inside the three-electrode assembly.

2.4. Fabrication of the w-NiS-3D-Nf and NiS-3D-Nf

The fabrication of three-dimensional hierarchically porous wrinkle-shaped NiS@Ni foam using a simple solvothermal method was as follows. The required moles of nickel chloride and thiourea were dissolved in a mixture of methanol and ethylene glycol solvent at a ratio of 20:5 mL. The mixture was stirred for 20 min. Next, two Ni foams were added and sonicated for a further 5 min. The solution and Ni foam were transferred into a Teflon lined autoclave at 115 °C for 10 h. Subsequently, reaction was completed and autoclave was cooled down at room temperature naturally. The synthesized electrodes were washed with DI water and ethanol several times to remove all ions and contamination remaining in fabricated electrode. The washed samples were dried in an oven at 80 °C for 24 h. The NiS grown on the 3D-Nf using methanol as solvent is abbreviated as NiS-3D-Nf. The NiS grown on the 3D-Nf using methanol and glycol as solvent mixture is abbreviated as w-NiS-3D-Nf (Figure 1).

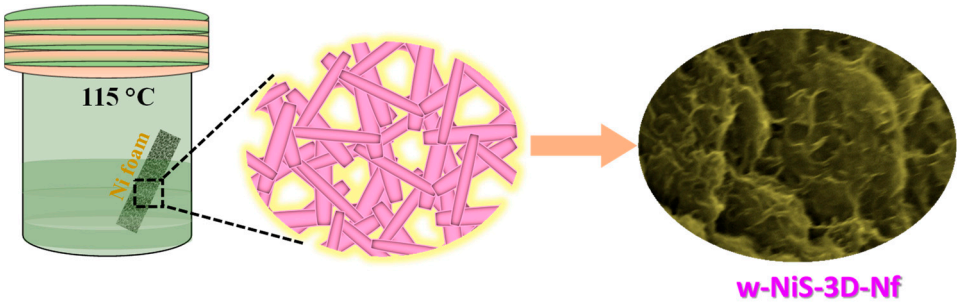

Figure 1. Schematic presentation of the preparation of the w-NiS-3D-Nf and NiS-3D-Nf electrode.

3. Results and Discussion

3.1. XRD Analysis

For synthesizing the nickel sulfides, we employed the one-step hydrothermal method, since it is an adaptable and appropriate method for controlling the material's morphology, structure, and phase, especially for inorganic materials. The optical images clearly show the change in the surface color of the 3D-Nf before and after hydrothermal treatment from slivery white to black, which was indicative of the new moieties successfully grown on the 3D-Nf. The crystallographic information of the as-prepared w-NiS-3D-Nf nanostructures was confirmed through an XRD analysis in the range of 2theta from 20 to 80 to identify the crystal and phase, as revealed in Figure 2. The XRD pattern peaks were observed at 2theta angles of 30.25, 34.85, 45.89, and 53.69, which can be well indexed to the crystal planes of (100), (101), (102), and (110). No extra diffraction peaks from the other phases were observed, suggesting the purity of the prepared w-NiS-3D-Nf sample. The prepared nanostructure was well-matched with the standard plane position of JCPDS card 10-075-0613.

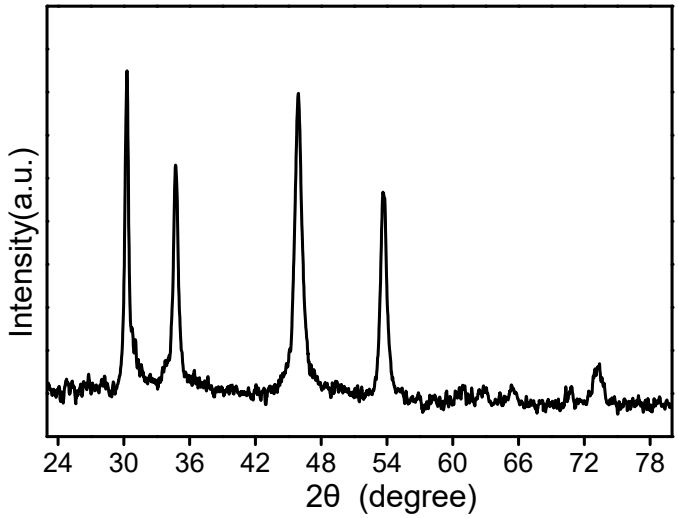

Figure 2. XRD pattern of the w-NiS-3D-Nf *electrode*.

3.2. SEM Analysis

The morphologies of the two-nickel sulfides grown directly onto the nickel foam using the different solvents in the solvothermal process are shown in Figure 3. In both cases, the active materials were uniformly deposited onto the conducting 3D nickel foam. Figure 3a,c,e,g represents the granular-shaped morphology of the NiS (NiS-3D-Nf) at different magnifications. Although the granular-shaped NiS was uniformly coated onto the surface of Ni foam, the low porosity and the presence of large cracks in the morphology may have resulted in the falling off the thin film during the charge–discharge processes, resulting in capacitance decay and decline in the cycling stability. On the other hand, a porous structure with interconnected channels was found to be highly desirable for

high-performance, binder-free electrodes [17–19]. Figure 3b,d,f,h represents the wrinkle-shaped NiS grown directly onto the nickel foam. The uniformly deposited 3D film with porosity and interconnected structure enabled the electrolyte ions to penetrate rapidly and smoothly to the active electrode materials, resulting in enhanced electrochemical performance [10,12,20]. The wrinkle-shaped porous and continuous crack-less structure provided extra stability to the binding of the active electrode material to the nickel foam and, therefore, the w-NiS-3D-Nf electrode outperformed the NiS-3D-Nf electrode.

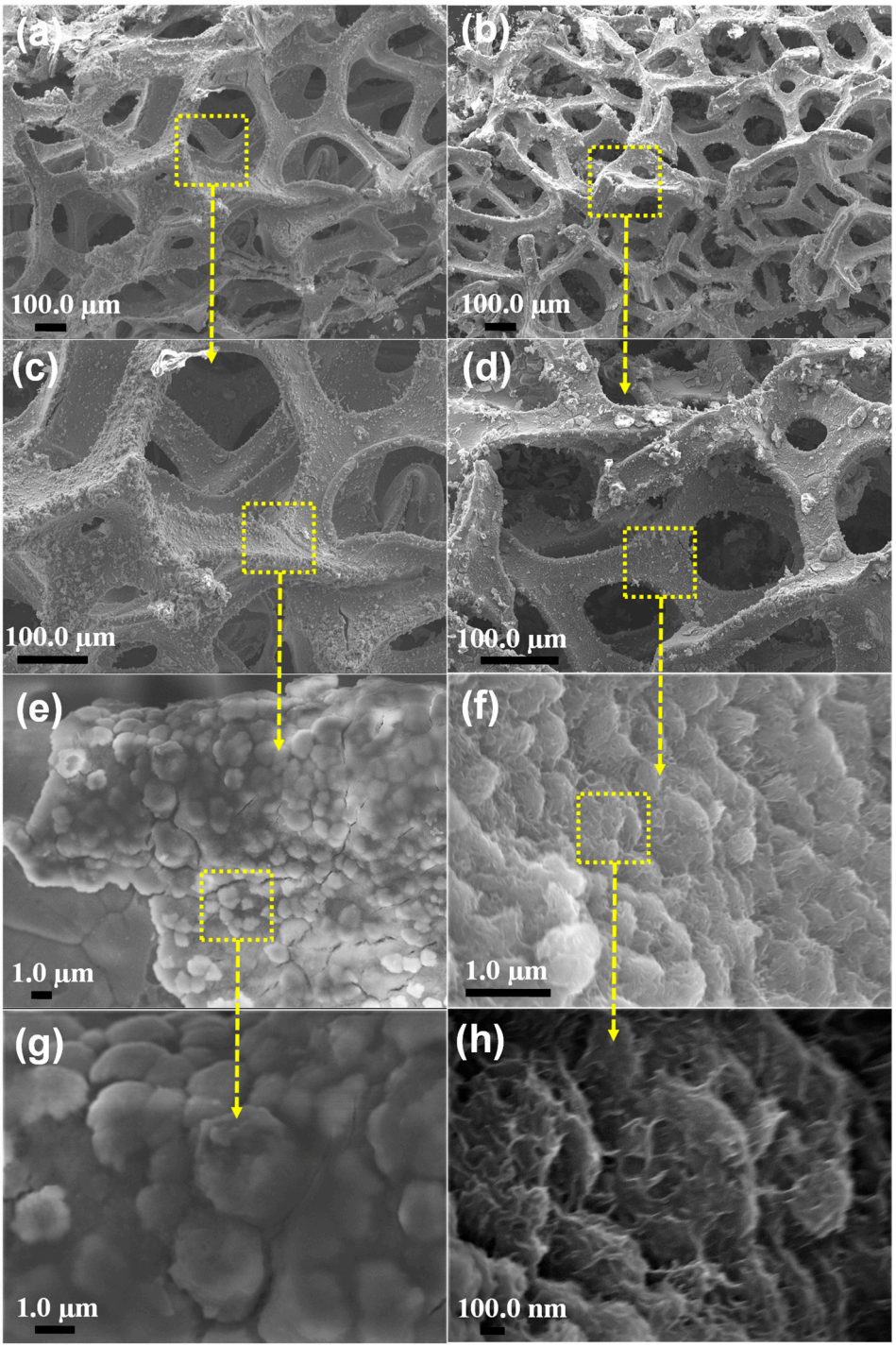

Figure 3. (**a**,**c**,**e**,**g**) FESEM images of the NiS-3D-Nf electrode at different magnifications and (**b**,**d**,**f**,**h**) FESEM images of the w-NiS-3D-Nf electrode at different magnifications.

3.3. XPS Analysis

A further confirmation of the good synthesis of the NiS electrode material wa performed by XPS analysis. The XPS technique was performed to determine the elemental composition and valence of the constituents in the finally synthesized material. Figure 4a represents the high-resolution XPS spectra of the nickel in the 2p state, centered at 855.30 eV for the Ni $2p_{3/2}$ state and 872.20 eV for the Ni $2p_{1/2}$ state. Furthermore, the two satellite peaks at 862.0 eV and 879.0 eV were in good agreement with the previous reported work on NiS [20,21]. Figure 4b shows the high-resolution XPS spectra of S, with the two peaks situated at 160.0 eV and 162.0 eV relating to the states $2p_{3/2}$ and $2p_{1/2}$, respectively, representing the presence of metal-sulfur bonds. In addition, the extra peak situated at 169.0 eV was due to the presence of sulfur on the surface of the material in the form of sulfates [22,23].

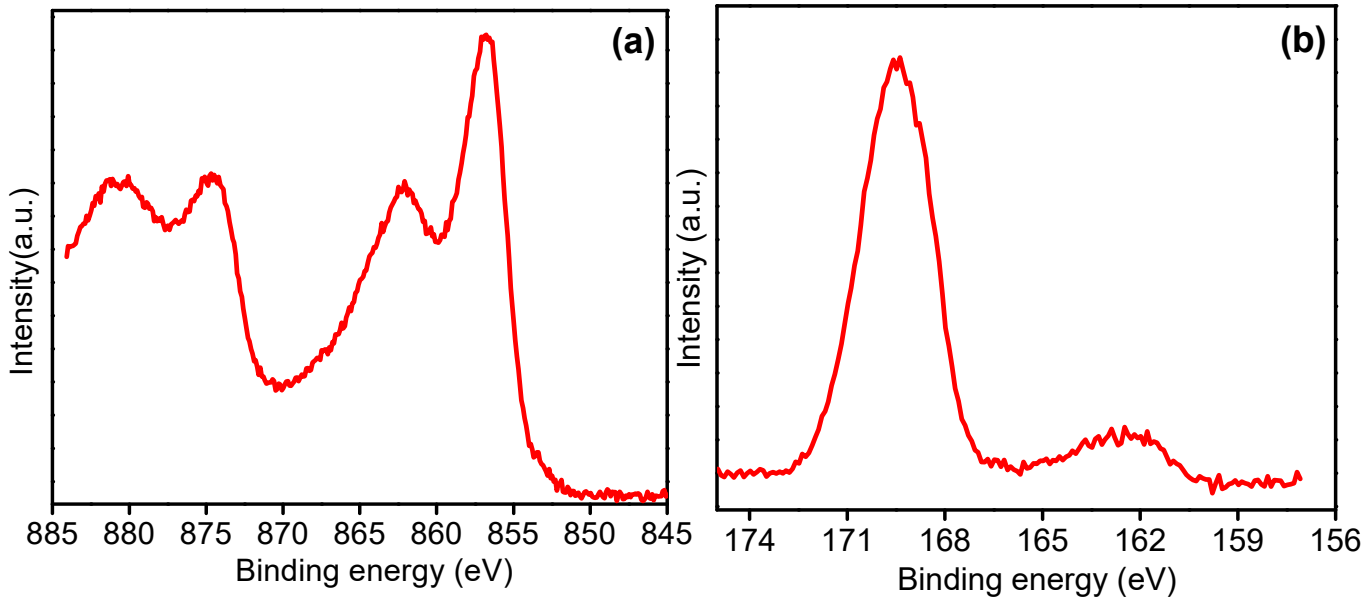

Figure 4. (**a**) Ni 2p XPS high-resolution spectra and (**b**) S 2p high-resolution spectra of the w-NiS-3D-Nf electrode.

3.4. Electrochemical Analysis

The supercapacitance performances of the w-NiS-3D-Nf and NiS-3D-Nf electrodes were evaluated through cyclic voltammetry (CV) and galvanostatic charge–discharge (GCD) measurements using a three-electrode cell-test system in a 2M aqueous KOH electrolyte medium. The CV test helps to determine the mechanism of the charge storage, while GCD technique determines the time taken by an electrode to become completely charged and discharged [17–24]. Figure 5a represents a comparison of the CV performances of the w-NiS-3D-Nf and NiS-3D-Nf electrodes at a fixed scan rate of 10 mV s^{-1} under the potential window of −0.1 to 0.4 V compared with the Ag/AgCl reference electrode. The CV curve profile demonstrates clearly that both the materials possessed well-defined redox peaks, indicating the pseudocapacitive nature of both the electrodes [25,26]. The redox reactions of the nickel sulfide in the aqueous KOH electrolyte is given as [27]:

$$NiS + OH^{-} \leftrightarrow NiSOH + e^{-} \quad (1)$$

The area under the CV curves represents the real specific capacitance of the electrodes [28,29]. In this study, among the two binder-free electrodes, the area enclosed by the CV curve of w-NiS-3D-Nf was larger than the NiS-3D-Nf electrode. Furthermore, the oxidation peak for the w-NiS-3D-Nf electrode had a higher potential than that of the NiS-3D-Nf electrode, showing the good reversibility and enhanced pseudocapacitance of the w-NiS-3D-Nf electrode compared to the NiS-3D-Nf electrode. Moreover, the GCD

test was carried out to determine the gravimetric specific capacitance of the fabricated 3D binder-free electrodes [30]. Figure 5b shows the GCD data plot of the w-NiS-3D-Nf and NiS-3D-Nf electrodes at a fixed current density of 1.0 Ag^{-1}. The non-linear GCD data profiles of both the samples show the resulting charge storage arising from faradaic redox reactions [31,32]. Although the chemical compositions of both the binder-free electrodes were the same, the different precursor solutions resulted in the NiS-based electrodes exhibiting different morphologies and, consequently, resulted in different electrochemical performances [1,12,20]. It is clear that the w-NiS-3D-Nf electrode took more time to discharge compared to the NiS-3D-Nf electrode and, therefore, possessed a higher gravimetric specific capacitance than the NiS-3D-Nf-based electrode. The specific capacitance of the electrodes is given by the following formula [12,13]:

$$C = \frac{Idt}{mdV} \quad (2)$$

where C represents the specific capacitance in Fg^{-1}, I is the current, t is the discharge time, m is the mass of the coated or loaded active materials, and dV represents the operating potential window [13]. From Equation (2), the gravimetric specific capacitance calculated for the w-NiS-3D-Nf binder-free electrode was found to be 770 Fg^{-1} at 1 Ag^{-1} of the current density, while for the NiS-3D-Nf, it was found to be 162.0 Fg^{-1} at the same current density (1 Ag^{-1}). The GCD data results also favored the CV data, which specified the enhanced electrochemical behavior of the w-NiS-3D-Nf electrode compared with the NiS-3D-Nf electrode. The obtained specific capacitance for the w-NiS-3D-Nf was found to be better than that of other NiS-based electrodes [33–37]. This could be attributed to the three-dimensional hierarchically porous wrinkle-shaped morphology having a large electroactive surface area, helping the electrolyte ions to access the maximum active area of the electrodes [38,39]. To further explore the charge–discharge behavior of the w-NiS-3D-Nf and NiS-3D-Nf electrodes, the GCD tests were carried out at different current densities, as shown in Figure 5c,d. The specific capacitance values determined for the NiS-3D-Nf electrode from Figure 5c at current densities of 1.0, 1.50, 2.0, 4.0, 6.0, and 8.0 Ag^{-1} were found to be 162.0 Fg^{-1}, 135.0 Fg^{-1}, 128.0 Fg^{-1}, 120.0 Fg^{-1}, 108.0 Fg^{-1}, and 64.0 Fg^{-1}, respectively, while for the w-NiS-3D-Nf electrode, from Figure 5d, at the similar current densities, the values were found to be 770.0 Fg^{-1}, 630.0 Fg^{-1}, 532.0 Fg^{-1}, 400.0 Fg^{-1}, 336.0 Fg^{-1}, and 112.0 Fg^{-1}, respectively. The remarkably enhanced specific capacitance of the w-NiS-3D-Nf electrode compared with the NiS-3D-Nf electrode calculated from the charge–discharge profiles, with obvious hysteresis, were due to the unique porosity of the wrinkled structure and the good adhesion of the active electrode material to the 3D nickel foam [40]. The porosity provided enough space for the electrolyte ions during the electrochemical reaction, whereas the three-dimensional structure facilitated faster ion and electron transport for the electrochemical reactions to occur via the conductive nickel foam.

A plot of the specific capacitance compared with the current density is shown in Figure 6a, which represents the higher rate capability of the w-NiS-3D-Nf binder-free electrode compared with the NiS-3D-Nf binder-free electrode. Cyclic stability over a large number of charge–discharge cycles is the most important parameter used to determine the performance of SC electrodes [41]. The consecutive charge and discharge cycling performance of the w-NiS-3D-Nf electrode is shown in Figure 6b, for 2200 consecutive cycles. The wrinkle-shaped, binder-free electrode retained 92.67% of its initial capacitance, demonstrating good capacitance retention over a long run. A slight fluctuation was observed during the consecutive charge and discharge cycling processes, which is normal in the case of the any developed electrodes. Thus, the cyclic performance also suggested the potential use of w-NiS-3D-Nf as a high-performance SC electrode. The wrinkle-shaped, unique w-NiS-3D-Nf electrode possesses an integrated hierarchical porous three-dimensional (3D) configuration, which facilitates faster ion and electron transport for electrochemical reactions to occur via the conductive nickel foam. The results obtained from the electrochemical tests also signify that the particular morphologies of active electrode materials has a direct

influence on electrochemical performance [42,43]. Thus, the w-NiS-3D-Nf binder-free electrode with a novel morphology provides better supercapacitance performance than the NiS-3D-Nf electrode.

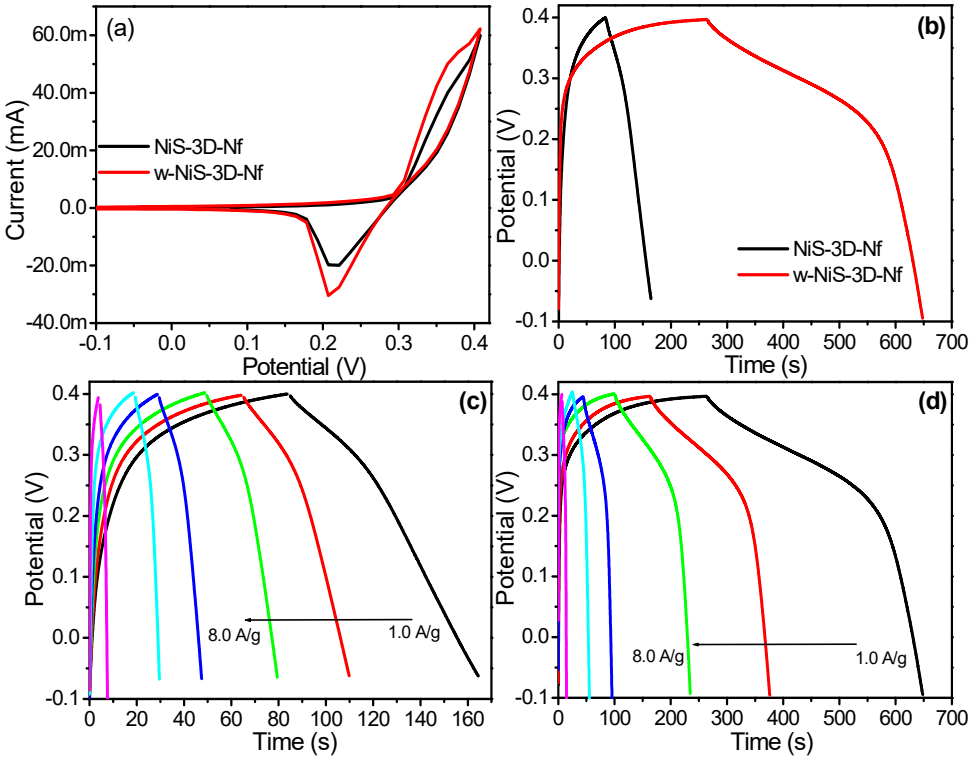

Figure 5. (**a**) Comparative CV graph of the w-NiS-3D-Nf and NiS-3D-Nf electrodes at a fixed scan rate of 10 mV s^{-1}, (**b**) comparison of the GCD profiles of the w-NiS-3D-Nf and NiS-3D-Nf electrodes at fixed current density of 1.0 Ag^{-1}, (**c**) comparison of the GCD profiles of the NiS-3D-Nf electrode at different current densities, and (**d**) w-NiS-3D-Nf electrode at different current densities.

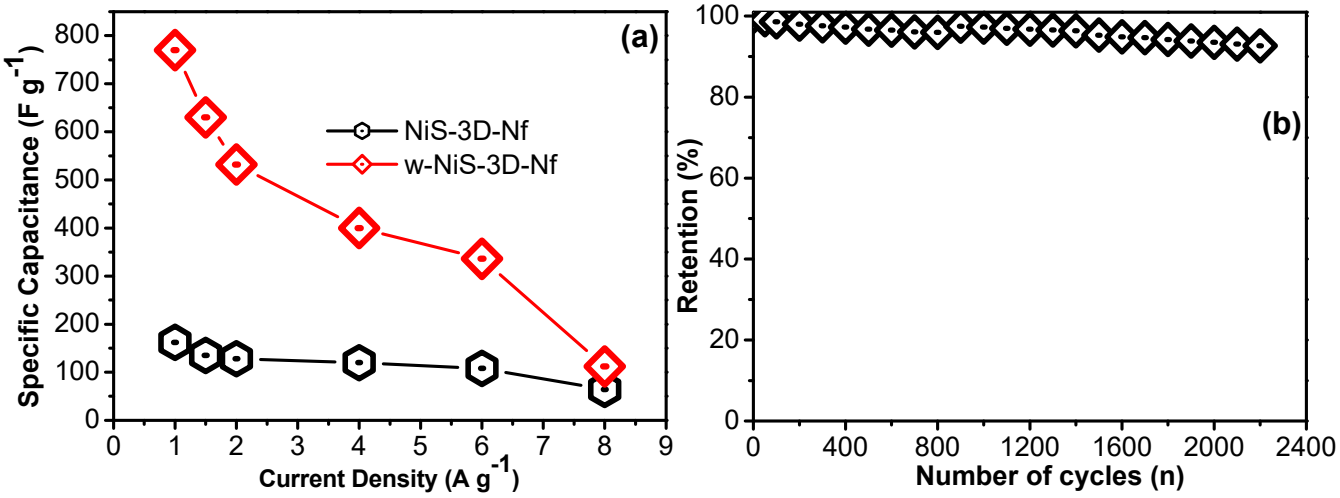

Figure 6. (**a**) Calculated specific capacitance of the NiS-3D-Nf and w-NiS-3D-Nf electrodes at different current densities and (**b**) cyclic stability graph of the w-NiS-3D-Nf electrode at a fixed current density.

4. Conclusions

A three-dimensional, hierarchically porous, wrinkle-shaped NiS and a nanogranular NiS were grown directly on a 3D-Nf substrate using a one-step solvothermal process. The developed electrodes, i.e., w-NiS-3D-Nf and NiS-3D-Nf, were characterized by the X-ray

diffraction pattern, X-ray photoelectron spectroscopy, and scanning electron microscopy techniques. The electrochemical performances of the individual electrodes were evaluated through the three-electrode assembly cell, in which the optimized w-NiS-3D-Nf electrode delivered an excellent specific capacitance, of 770 Fg^{-1}, compared with the NiS-3D-Nf electrode (162.0 Fg^{-1}), at a current density of 1.0 Ag^{-1} and with a cyclic stability of over 92.67% capacitance retention after 2200 cycles. The resultant unique structure, with an integrated hierarchical three-dimensional configuration can not only enhance abundant accessible surface areas but also produce strong adhesion to the 3D-Nf, facilitating the fast transportation of ions and electrons for electrochemical reactions via the conductive substrate. These results suggest that the modification of 3D-Nf surfaces with suitable solvents has highly significant effects on morphology, and ultimately, electrochemical performance.

Author Contributions: Conceptualization, S.A.A. and H.M.K.; methodology, S.A.A.; software, H.M.K.; validation, S.A.A., H.M.K. and M.M.A., formal analysis, M.M.A.; investigation, S.A.A., H.M.K. and M.M.A.; resources, S.A.A., H.M.K. and M.M.A.; data curation, S.A.A., H.M.K. and M.M.A.; writing—original draft preparation, S.A.A., H.M.K. and M.M.A.; writing—review and editing, M.M.A. and H.M.K.; visualization, M.M.A.; supervision, S.A.A., H.M.K. and M.M.A.; project administration, H.M.K.; funding acquisition, S.A.A., H.M.K. and M.M.A. All authors have read and agreed to the published version of the manuscript.

Funding: This research was funded by the Deanship of Scientific Research at King Faisal University (Saudi Arabia), grant number 1811017, and the APC was funded by the same grant number, 1811017.

Institutional Review Board Statement: Not applicable.

Informed Consent Statement: Not applicable.

Data Availability Statement: Not applicable.

Acknowledgments: The authors acknowledge the Deanship of Scientific Research at King Faisal University (Saudi Arabia) for financial support on the Research Group Support Track (grant no. 1811017).

Conflicts of Interest: The authors declare no conflict of interest.

References

1. Parveen, N.; Ansari, S.A.; Ansari, M.Z.; Ansari, M.O. Manganese oxide as an effective electrode material for energy storage: A review. *Environ. Chem. Lett.* **2022**, *20*, 283–309. [CrossRef]
2. Ansari, M.Z.; Parveen, N.; Nandi, D.K.; Ramesh, R.; Ansari, S.A.; Cheon, T.; Kim, S.H. Enhanced activity of highly conformal and layered tin sulfide (SnSx) prepared by atomic layer deposition (ALD) on 3D metal scaffold towards high performance supercapacitor electrode. *Sci. Rep.* **2019**, *9*, 10225. [CrossRef] [PubMed]
3. Ansari, M.Z.; Nandi, D.K.; Janicek, P.; Ansari, S.A.; Ramesh, R.; Cheon, T.; Shong, B.; Kim, S.-H. Low-temperature atomic layer deposition of highly conformal tin nitride thin films for energy storage devices. *ACS Appl. Mater. Interfaces* **2019**, *11*, 43608–43621. [CrossRef] [PubMed]
4. Yu, M.; Chen, J.; Liu, J.; Li, S.; Ma, Y.; Zhang, J.; An, J. Mesoporous $NiCo_2O_4$ nanoneedles grown on 3D graphene-nickel foam for supercapacitor and methanol electro-oxidation. *Electrochim. Acta* **2015**, *151*, 99–108. [CrossRef]
5. Liu, L.; Zhao, H.; Lei, Y. Advances on three-dimensional electrodes for micro-supercapacitors: A mini-review. *InfoMat* **2019**, *1*, 74–84. [CrossRef]
6. Faraji, S.; Ani, F.N. Microwave-assisted synthesis of metal oxide/hydroxide composite electrodes for high power supercapacitors—A review. *J. Power Sources* **2014**, *263*, 338–360. [CrossRef]
7. Shaikh, S.; Rabinal, M.K. Facile one-step growth of nickel sulfide nano-architecture as binder less electrodes for efficient supercapacitor applications. *Mater. Sci. Semicond. Processing* **2022**, *142*, 106524. [CrossRef]
8. Yu, L.; Yang, B.; Liu, Q.; Liu, J.; Wang, X.; Song, D.; Wang, J.; Jing, X. Interconnected NiS nanosheets supported by nickel foam: Soaking fabrication and supercapacitors application. *J. Electroanal. Chem.* **2015**, *739*, 156–163. [CrossRef]
9. Ho, K.; Lin, L. A review of electrode materials based on core–shell nanostructures for electrochemical supercapacitors. *J. Mater. Chem. A* **2019**, *7*, 3516–3530. [CrossRef]
10. Khalid, S.; Khan, Y.; Ahmed, E.; Nawaz, S.; Khalid, N.R.; Ahmed, W. Chapter 16—Transition metal sulfides for supercapacitors. In *Micro and Nano Technologies, Emerging Nanotechnologies for Renewable Energy*; Ahmed, W., Booth, M., Nourafkan, E., Eds.; Elsevier: Amsterdam, The Netherlands, 2021; pp. 407–445.
11. Akhtar, M.S.; Gul, I.H.; Baig, M.M.; Akram, M.A. Binder-free pseudocapacitive nickel cobalt sulfide/MWCNTs hybrid electrode directly grown on nickel foam for high rate supercapacitors. *Mater. Sci. Eng. B* **2021**, *264*, 114898. [CrossRef]

12. Parveen, N.; Ansari, S.A.; Ansari, S.G.; Fouad, H.; Salam, N.M.; Cho, M.H. Solid-state symmetrical supercapacitor based on hierarchical flower-like nickel sulfide with shape-controlled morphological evolution. *Electrochim. Acta* **2018**, *268*, 82–93. [CrossRef]
13. Ansari, S.A.; Parveen, N.; Alothoum, M.A.S.; Ansari, M.O. Development of binder free interconnected 3D flower of NiZn2O4 as an advanced electrode materials for supercapacitor Applications. *Crystals* **2022**, *12*, 14. [CrossRef]
14. Liu, B.; Zhang, J.; Wang, X.; Chen, G.; Chen, D.; Zhou, C.; Shen, G. Hierarchical Three-Dimensional $ZnCo_2O_4$ Nanowire Arrays/Carbon Cloth Anodes for a Novel Class of High-Performance Flexible Lithium-Ion Batteries. *Nano Lett.* **2012**, *12*, 3005–3011. [CrossRef] [PubMed]
15. Zhang, G.Q.; Wu, H.B.; Hoster, H.E.; Chan-Park, M.B.; Lou, X.W. Single-crystalline $NiCo_2O_4$ nanoneedle arrays grown on conductive substrates as binder-free electrodes for high-performance supercapacitors. *Energy Environ. Sci.* **2012**, *5*, 9453–9456. [CrossRef]
16. Rahman, M.A.; Rahman, M.M.; Song, G. A review on binder-free NiO-Ni foam as anode of high performance lithium-ion batteries. *Energy Storage* **2021**, e278, in press. [CrossRef]
17. Noémie, E.; Rountree, K.J.; McCarthy, B.D.; Rountree, E.S.; Eisenhart, T.T.; Dempsey, J.L. A practical beginner's guide to cyclic voltammetry. *J. Chem. Educ.* **2018**, *95*, 197–206.
18. Stoller, M.D.; Ruoff, R.S. Best practice methods for determining an electrode material's performance for ultracapacitors. *Energy Environ. Sci.* **2010**, *3*, 1294–1301. [CrossRef]
19. Aderyani, S.; Flouda, P.; Shah, S.A.; Green, M.J.; Lutkenhaus, J.L.; Ardebili, H. Simulation of cyclic voltammetry in structural supercapacitors with pseudocapacitance behavior. *Electrochim. Acta* **2021**, *390*, 138822. [CrossRef]
20. Ouyang, Y.; Chen, Y.; Peng, J.; Yang, J.; Wu, C.; Chang, B.; Guo, X.; Chen, G.; Luo, Z.; Wang, X. Nickel sulfide/activated carbon nanotubes nanocomposites as advanced electrode of high-performance aqueous asymmetric supercapacitors. *J. Alloys Compd.* **2021**, *885*, 160979. [CrossRef]
21. Niu, W.; Xiao, Z.; Wang, S.; Zhai, S.; Qin, L.; Zhao, Z.; An, Q. Synthesis of nickel sulfide-supported on porous carbon from a natural seaweed-derived polysaccharide for high-performance supercapacitors. *J. Alloys Compd.* **2021**, *853*, 157123. [CrossRef]
22. Li, X.; Yan, W.; Guo, S.; Liu, Y.; Niu, J.; Yin, L.; Wang, Z. One-step electrochemical controllable preparation of nickel cobalt sulfide nanosheets and its application in supercapacitors. *Electrochim. Acta* **2021**, *387*, 138488. [CrossRef]
23. Hu, Q.; Zhang, S.; Zou, X.; Hao, J.; Bai, Y.; Yan, L.; Li, W. Coordination agent-dominated phase control of nickel sulfide for high-performance hybrid supercapacitor. *J. Colloid Interface Sci.* **2022**, *607*, 45–52. [CrossRef] [PubMed]
24. Iqbal, M.F.; Yousef, A.K.M.; Hassan, A.; Hussain, S.; Ashiq, M.N.; Razaq, A. Significantly improved electrochemical characteristics of nickel sulfide nanoplates using graphene oxide thin film for supercapacitor applications. *J. Energy Storage* **2021**, *33*, 102091. [CrossRef]
25. Peng, L.; Ji, X.; Wan, H.; Ruan, Y.; Xu, K.; Chen, C.; Miao, L.; Jiang, J. Nickel sulfide nanoparticles synthesized by microwave-assisted method as promising supercapacitor electrodes: An experimental and computational study. *Electrochim. Acta* **2015**, *182*, 361–367. [CrossRef]
26. Naveenkumar, P.; Kalaignan, G.P. Electrodeposited MnS on graphene wrapped Ni-Foam for enhanced supercapacitor applications. *Electrochim. Acta* **2018**, *289*, 437–447. [CrossRef]
27. Marand, N.A.; Masoudpanah, S.M.; Alamolhoda, S.; Bafghi, M.S. Solution combustion synthesis of nickel sulfide/reduced graphene oxide composite powders as electrode materials for high-performance supercapacitors. *J. Energy Storage* **2021**, *39*, 102637. [CrossRef]
28. Huang, H.; Deng, X.; Yan, L.; Wei, G.; Zhou, W.; Liang, X.; Guo, J. One-step synthesis of self-supported Ni_3S_2/NiS composite film on Ni foam by electrodeposition for high-performance supercapacitors. *Nanomaterials* **2019**, *9*, 1718. [CrossRef]
29. Kumar, M.; Jeong, D.I.; Sarwar, N.; Yoon, D.H. Heazlewoodite, Ni_3S_2: An electroactive material for supercapacitor application. *Ceram. Int.* **2021**, *47*, 16852–16860. [CrossRef]
30. El-Gendy, D.M.; Afifi, I.M.; Allam, N.K. Eco-friendly, one-step synthesis of cobalt sulfide-decorated functionalized graphene for high-performance supercapacitors. *J. Energy Storage* **2019**, *24*, 100760. [CrossRef]
31. Wang, F.; Li, G.; Zheng, J.; Ma, J.; Yang, C.; Wang, Q. Microwave synthesis of three-dimensional nickel cobalt sulfide nanosheets grown on nickel foam for high-performance asymmetric supercapacitors. *J. Colloid Interface Sci.* **2018**, *516*, 48–56. [CrossRef]
32. Saddique, J.; Cheng, X.; Shi, H.; Wu, R.; Zhang, Y. High-performance Ni-Co sulfide nanosheet-nanotubes grown on Ni Foam as a binder free electrode for supercapacitors. *Appl. Sci.* **2019**, *9*, 3082. [CrossRef]
33. Mun, C.-H.; Gopi, C.V.V.M.; Vinodh, R.; Sambasivam, S.; Obaidat, I.M.; Kim, H.J. Microflower-like nickel sulfide-lead sulfide hierarchical composites as binder-free electrodes for high-performance supercapacitors. *J. Energy Storage* **2019**, *26*, 100925. [CrossRef]
34. Gou, J.; Xie, S.; Li, Y.; Kong, X.; Li, C. Studies on preparation and performance of nickel sulfides for the application in supercapacitors. *J. Mater. Sci. Mater. Electron.* **2019**, *30*, 15429–15436. [CrossRef]
35. Li, Y.; Ye, K.; Cheng, K.; Yin, J.; Cao, D.; Wang, G. Electrodeposition of nickel sulfide on graphene-covered make-up cotton as a flexible electrode material for high-performance supercapacitors. *J. Power Sources* **2015**, *274*, 943–950. [CrossRef]
36. Xue, G.; Bai, T.; Wang, W.; Wang, S.; Ye, M. Recent advances in various applications of nickel cobalt sulfide-based materials. *J. Mater. Chem. A* **2022**, *10*, 8087–8106. [CrossRef]

37. Singh, A.; Roberts, A.J.; Slade, R.C.T.; Chandra, A. High electrochemical performance in asymmetric supercapacitors using MWCNT/nickel sulfide composite and graphene nanoplatelets as electrodes. *J. Mater. Chem. A* **2014**, *2*, 16723–16730. [CrossRef]
38. Bhagwan, J.; Hussain, S.K.; Krishna, B.N.V.; Yu, J.S. β-NiS 3D micro-flower-based electrode for aqueous asymmetric supercapacitors. *Sustain. Energy Fuels* **2020**, *4*, 5550–5559. [CrossRef]
39. Darsara, S.A.; Seifi, M.; Askari, M.B.; Osquian, M. Hierarchical 3D starfish-like Ni_3S_4–NiS on reduced graphene oxide for high-performance supercapacitors. *Ceram. Int.* **2021**, *47*, 20992–20998. [CrossRef]
40. Ahmed, N.; Ali, B.A.; Ramadan, M.; Allam, N.K. Three-dimensional interconnected binder-free Mn–Ni–S nanosheets for high performance asymmetric supercapacitor devices with exceptional cyclic stability. *ACS Appl. Energy Mater.* **2019**, *2*, 3717–3725. [CrossRef]
41. Paliwal, M.K.; Meher, S.K. $Co_3O_4/NiCo_2O_4$ perforated nanosheets for high-energy-density all-solid-state asymmetric supercapacitors with extended cyclic stability. *ACS Appl. Nano Mater.* **2020**, *3*, 4241–4252. [CrossRef]
42. Hu, Q.; Li, W.; Xiang, B.; Zou, X.; Hao, J.; Deng, M.; Wu, Q.; Wang, Y. Sulfur source-inspired synthesis of β-NiS with high specific capacity and tunable morphologies for hybrid supercapacitor. *Electrochim. Acta* **2020**, *337*, 135826. [CrossRef]
43. Chen, L.; Guan, L.; Tao, J. Morphology control of Ni_3S_2 multiple structures and their effect on supercapacitor performances. *J. Mater. Sci.* **2019**, *54*, 12737–12746. [CrossRef]